Deviation-angle and trajectory statistics for inertial particles in turbulence

Akshay Bhatnagar,[1,2,*] Anupam Gupta,[3,†] Dhrubaditya Mitra,[2,‡] Prasad Perlekar,[4,§]
Michael Wilkinson,[5,‖] and Rahul Pandit[1,¶]

[1]*Centre for Condensed Matter Theory, Department of Physics, Indian Institute of Science, Bangalore 560012, India*
[2]*Nordita, KTH Royal Institute of Technology and Stockholm University, Roslagstullsbacken 23, 10691 Stockholm, Sweden*
[3]*Laboratoire de Génie Chimique, FERMAT, Université de Toulouse, INPT-UPS, 31030, Toulouse, France*
[4]*TIFR Centre for Interdisciplinary Sciences, 21 Brundavan Colony, Narsingi, Hyderabad 500075, India*
[5]*Department of Mathematics and Statistics, The Open University, Milton Keynes MK6 7AA, United Kingdom*

(Received 19 June 2016; published 23 December 2016)

Small particles in suspension in a turbulent fluid have trajectories that do not follow the pathlines of the flow exactly. We investigate the statistics of the angle of deviation ϕ between the particle and fluid velocities. We show that, when the effects of particle inertia are small, the probability distribution function (PDF) P_ϕ of this deviation angle shows a power-law region in which $P_\phi \sim \phi^{-4}$. We also find that the PDFs of the trajectory curvature κ and modulus θ of the torsion ϑ have power-law tails that scale, respectively, as $P_\kappa \sim \kappa^{-5/2}$, as $\kappa \to \infty$, and $P_\theta \sim \theta^{-3}$, as $\theta \to \infty$: These exponents are in agreement with those previously observed for fluid pathlines. We propose a way to measure the complexity of heavy-particle trajectories by the number $N_{\rm I}(t,{\rm St})$ of points (up until time t) at which the torsion changes sign. We present numerical evidence that $n_{\rm I}({\rm St}) \equiv \lim_{t\to\infty} \frac{N_{\rm I}(t,{\rm St})}{t} \sim {\rm St}^{-\Delta}$ for large St, with $\Delta \simeq 0.5$.

DOI: 10.1103/PhysRevE.94.063112

Small particles in suspension in a turbulent flow play an important role in many geophysical [1], atmospheric [2,3], astrophysical [4], and industrial processes [5,6]. The theoretical difficulties in understanding these systems are reviewed in [7,8]. Experimental, theoretical, and especially numerical investigations, which have been carried out over the past few decades, have shown that neutrally buoyant tracers (or Lagrangian particles) respond very differently to turbulent flows than do heavy inertial particles [9,10]; for instance, tracers get distributed uniformly in space in a turbulent incompressible flow, but, in the same flow, heavy inertial particles cluster [11,12], especially when the Stokes number ${\rm St} \simeq 1$, where ${\rm St} = \tau_{\rm s}/\tau_\eta$, with $\tau_{\rm s}$ the particle-response or Stokes time and τ_η the Kolmogorov time, at the dissipation length scale η. We address an aspect of the particle motion that has not been featured in earlier investigations. Suspended particles in a turbulent fluid are often used to image the flow. If the particles are extremely small tracers, they follow the flow exactly, but when solid particles or liquid droplets are suspended in a gas, inertial effects can be significant. Here we investigate the probability distribution of the angle between the velocity of the fluid $\boldsymbol{u}$ and the velocity of a suspended particle $\boldsymbol{v}$. We also characterize the geometry of the particle trajectories by obtaining statistical properties of their curvature and torsion.

Our theoretical and numerical studies of these statistical properties yield universal scaling exponents that characterize heavy-particle trajectories. In particular, we consider three quantities: the deviation angle ϕ, the angle between the particle velocity $\boldsymbol{v}$ and the Eulerian velocity $\boldsymbol{u}(\boldsymbol{x},t)$ at the position $\boldsymbol{x}$ of the particle at time t; the curvature κ; and the torsion ϑ (with $\theta = |\vartheta|$) of the trajectories of the particles. We find from direct numerical simulations (DNSs) that when the Stokes number is small, the probability distribution function (PDF) of ϕ shows a power-law region in which $P_\phi \sim \phi^{-4}$. The extent of this power-law regime decreases as St increases. We find good power-law fits if $0 < {\rm St} \lesssim 0.7$; in this range the exponent is universal inasmuch as its values for different St and Re (the fluid Reynolds number) lie within error bars of each other. We also find that the PDFs of κ and $\theta = |\vartheta|$ show power-law tails for large κ and θ, respectively. In this case the exponents are the same as previously reported for fluid pathlines, namely, $P_\kappa \sim \kappa^{-5/2}$ and $P_\theta \sim \theta^{-3}$ (see [13–15]). We also present a theory for the exponents that characterize the tails of the PDFs P_ϕ, P_κ, and P_θ; this theory complements our DNS results. Finally, we attempt to quantify the complexity of particle trajectories by calculating $N_{\rm I}(t,{\rm St})$, the number of points along the particle trajectories at which the torsion changes sign per unit time. We present numerical evidence that this number scales as $\frac{N_{\rm I}}{t} \sim {\rm St}^{-\Delta}$, as ${\rm St} \to \infty$, with $\Delta \simeq 0.5$.

We perform a DNS [16] of the incompressible three-dimensional (3D) forced Navier-Stokes equation

$$D_t \boldsymbol{u} = \nu \nabla^2 \boldsymbol{u} - \boldsymbol{\nabla} p + \boldsymbol{f}, \tag{1}$$

$$\boldsymbol{\nabla} \cdot \boldsymbol{u} = 0, \tag{2}$$

where $\boldsymbol{u}$, p, $\boldsymbol{f}$, and ν are the velocity, pressure, external force, and kinematic viscosity, respectively, and the fluid density $\rho_{\rm f}$ is chosen to be 1; the Lagrangian derivative is $D_t \equiv \partial_t + \boldsymbol{u} \cdot \boldsymbol{\nabla}$. Our simulation domain is a periodic cubical box with sides of length 2π (see Table I). The external force maintains a constant rate of energy injection [17,18], which is equal to the energy-dissipation rate ε in the statistically stationary state of turbulence. We use a second-order exponential Adams-Bashforth method of time stepping and pseudospectral method with a two-thirds dealiasing rule [16] for spatial derivatives.

*akshayphy@gmail.com
†anupam1509@gmail.com
‡dhruba.mitra@gmail.com
§perlekar@tifrh.res.in
‖m.wilkinson@open.ac.uk
¶rahul@physics.iisc.ernet.in

TABLE I. Parameters for our runs R1 and R2 with $\mathcal{N}^3$ collection points, ν the coefficient of kinematic viscosity, δt the time step, $\mathcal{N}_\mathrm{p}$ the number of particles, k_max the largest wave number in the simulation, η and τ_η the dissipation length and time scales, respectively, λ the Taylor microscale, Re_λ the Taylor-microscale Reynolds number, L_I the integral length scale, and T_eddy the large-eddy turnover time.

Run	$\mathcal{N}$	ν	δt	$\mathcal{N}_\mathrm{p}$	Re_λ	$k_\mathrm{max}\eta$	ε	η	λ	L_I	τ_η	T_eddy
R1	256	3.8×10^{-3}	5×10^{-4}	40 000	43	1.56	0.49	1.82×10^{-2}	0.16	0.51	8.76×10^{-2}	0.49
R2	512	1.2×10^{-3}	2×10^{-4}	100 000	79	1.21	0.69	7.1×10^{-3}	0.08	0.47	4.18×10^{-2}	0.41

We consider monodisperse spherical particles whose radii r_p are significantly smaller than the Kolmogorov scale of the fluid. We assume, furthermore, that the material density ρ_p of each particle is significantly larger than ρ_f and that the number density of the particles is small. In this parameter regime, we can ignore the backreaction from the particles to the flow (passive-particle approximation) and also particle-particle interactions. Hence, the equations of motion of each individual particle are [19,20]

$$\dot{\boldsymbol{X}} = \boldsymbol{v}, \quad \dot{\boldsymbol{v}} = \frac{1}{\tau_\mathrm{s}}\{\boldsymbol{u}[\boldsymbol{X}(t),t] - \boldsymbol{v}\}, \tag{3}$$

where $\boldsymbol{X}$ and $\boldsymbol{v}$ are the position and velocity of a particle, respectively, and the Stokes time $\tau_\mathrm{s} \equiv 2r_\mathrm{p}^2\rho_\mathrm{p}/9\nu\rho_\mathrm{f}$. The particles that obey (3) are called heavy inertial particles. We solve Eq. (3) by using an Euler scheme in time. To find out the flow velocity at the (off-grid) position of the particles we use trilinear interpolation.

A particle trajectory is a 3D curve that we characterize via the usual techniques of differential geometry [13,21,22] by its tangent $\boldsymbol{T}$, normal $\boldsymbol{N}$, and binormal $\boldsymbol{B}$. As a function of the arc length of this trajectory, $\boldsymbol{T}$, $\boldsymbol{N}$, and $\boldsymbol{B}$ together satisfy the Frenet-Serret equations. We illustrate the geometry of a particle trajectory by the sketch in Fig. 1(a).

First, consider how to determine the PDF of the angle ϕ between $\boldsymbol{v}$ and $\boldsymbol{u}$. If $\boldsymbol{w} = \boldsymbol{u} - \boldsymbol{v}$ and $w_\perp$ is the magnitude of the component of $\boldsymbol{w}$ that is perpendicular to $\boldsymbol{v}$, then $\sin\phi = w_\perp/u$ where $u = |\boldsymbol{u}|$. We use the small-angle approximation $\phi \sim w_\perp/u$. Hence, the PDF of ϕ can be obtained from the joint PDF of u and $\boldsymbol{w}$. Equation (3) implies that the particle acceleration $\boldsymbol{a} = \dot{\boldsymbol{v}}$ is related to $\boldsymbol{w}$ by $\tau_\mathrm{s}\boldsymbol{a} = \boldsymbol{w}$. For small τ_s, the acceleration of the particle and the fluid at the same point are approximately equal. By putting these elements together, we obtain $\phi \approx \tau_\mathrm{s}a_N^\mathrm{f}/u$, where a_N^f is the component of the fluid acceleration along $\boldsymbol{N}$. These approximations are valid for small ϕ and small τ_s. Hence, the PDF of ϕ can be written as follows:

$$P_\phi = \int \delta\left(\phi - \frac{\tau_\mathrm{s}a_N^\mathrm{f}}{u}\right)\mathcal{P}_\mathrm{au}^\mathrm{f}(a_N^\mathrm{f},u)\,da_N^\mathrm{f}\,du, \tag{4}$$

where $\delta(\cdot)$ is the Dirac delta function and $\mathcal{P}_\mathrm{au}^\mathrm{f}(a_N^\mathrm{f},u)$ is the joint PDF of a_N^f and u. Next we assume that this joint PDF factorizes, i.e.,

$$\mathcal{P}_\mathrm{au}^\mathrm{f}(a_N^\mathrm{f},u) \sim P_\mathrm{a}^\mathrm{f}(a_N^\mathrm{f})P_\mathrm{u}(u), \tag{5}$$

where P_a^f is the PDF of a_N^f and P_u is the PDF of u. We justify the assumption (5), within the framework of the Kolmogorov theory [23,24], which assumes that the only information about large-scale properties of the flow that is relevant to small-scale features is the rate of dissipation ε. The smallest-scale motions may also depend upon the kinematic viscosity ν and dimensional arguments [23,24] then imply that the typical acceleration because of small-scale eddies is $a_* = \varepsilon^{3/4}\nu^{-1/4}$, whereas the typical velocity because of small-scale eddies is $u_\mathrm{K} = \frac{\eta}{\tau_\mathrm{s}} = (\varepsilon\nu)^{1/4}$. In the limit of large Reynolds number, these estimates indicate that a_* is much larger than the typical accelerations because of the large-scale motion of the fluid, whereas u_K is much smaller than the large-scale velocities. We can conclude that, when the Reynolds number is large, a_N^f is determined by small-scale properties of the flow, whereas u is determined by large-scale motions. The hypotheses of

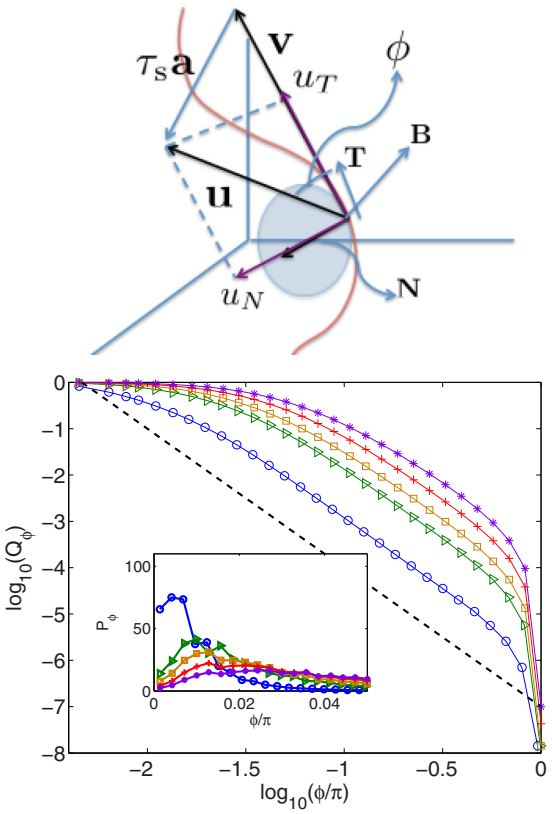

FIG. 1. Shown on top is a schematic illustration of the trajectory of a particle (shown in red). The particle velocity $\boldsymbol{v}$ is tangent to this trajectory. The circle is the osculating circle whose radius gives the radius of curvature. The three units vectors $\boldsymbol{T}$, $\boldsymbol{N}$, and $\boldsymbol{B}$ are the tangent, normal, and the binormal, respectively. The flow velocity is $\boldsymbol{u}$ and the deviation angle between $\boldsymbol{u}$ and $\boldsymbol{v}$ is ϕ. On the bottom are cumulative PDFs Q_ϕ of the deviation angle ϕ for St = 0.2 (blue circles), St = 0.5 (green triangles), St = 0.7 (brown squares), St = 1.0 (red pluses), and St = 1.4 (purple stars), obtained, by using the rank-order method, from our DNS. The slope of the black dashed line is −3. The inset shows plots of the PDF P_ϕ from our DNS.

the Kolmogorov theory then indicate that these quantities are independent, justifying (5). We also need to identify the forms of the distributions $P_{\rm u}$ and $P_{\rm a}^{\rm f}$. Data from DNSs and experiments are consistent with the Maxwellian form $P_{\rm u} \simeq C u^{d-1} \exp(-u^2/u_0^2)$, where $d = 3$ is the dimension of space, C is a normalization constant, and u_0 is the characteristic scale of flow velocities. We use this Maxwellian form and obtain, by integrating (4) over u,

$$P_\phi \sim C\phi^{-(d+1)}\tau_{\rm s}^d \int P_{\rm a}^{\rm f}(y) y^d \exp\left[-\frac{\tau_{\rm s}^2 y^2}{\phi^2 u_0^2}\right] dy. \qquad (6)$$

The PDF of the fluid acceleration decreases very rapidly for large values of its arguments [25]. Hence we can assume that $P_{\rm a}^{\rm f}(y)$ is negligible for $y \gg a_*$, where a_* is the characteristic scale of acceleration. Let $\phi_* \equiv \tau_{\rm s} a_*/u_0 \sim {\rm St}/{\rm Re}^{1/4}$. For $\phi \gg \phi_*$, the exponential factor in (6) is unity, so

$$P_\phi \sim C\phi^{-(d+1)}\tau_{\rm s}^d \langle (a_N^{\rm f})^d \rangle, \qquad (7)$$

where $\langle\cdot\rangle$ denotes the average over the statistically steady state of our system. Thus, for $d = 3$, we expect $P_\phi \sim \phi^{-4}$; for $\phi \ll 1$, small $\tau_{\rm s}$; and for $\phi \gg \phi_*$, $\phi_* \sim {\rm St}/{\rm Re}^{1/4}$. Note that this power-law range is present only if $\phi_* \ll 1$, which can be satisfied for small St and large Re [26].

To confront our theory with data from our DNS, we plot P_ϕ as an inset in Fig. 1(b) for several different values of St. Numerical calculations of PDFs by constructing histograms are often plagued by binning errors. To avoid such errors, we construct the cumulative PDF ($Q_\phi = \int_\phi^\infty P_\phi d\phi$) of ϕ by using the rank-order method [27] and plot Q_ϕ for several values of St in Fig. 1(b). For small-enough St, we obtain a clear range over which $Q_\phi \sim \phi^{-3}$. In addition to this clear agreement between our theory and DNS data, experimental evidence also supports our theory [28].

Let us now turn to curvature and torsion along particle trajectories, which are defined by

$$\kappa = \frac{a_N}{v^2}, \quad \vartheta = \frac{\boldsymbol{v}\cdot(\dot{\boldsymbol{v}}\times\ddot{\boldsymbol{v}})}{\kappa^2 v^6}. \qquad (8)$$

The PDFs of the curvature and torsion of the trajectories of passive *tracer* (superscript tr) particles $P_\kappa^{\rm tr}$ and $P_\theta^{\rm tr}$, respectively, have already been shown, from theory [14,15], DNS [13,15], and experiments [14], to have the following power-law tails: $P_\kappa^{\rm tr} \sim \kappa^{-5/2}$ as $\kappa \to \infty$ and $P_\theta^{\rm tr} \sim \theta^{-3}$ as $\theta \to \infty$. The theory of these exponents, as described in Refs. [14,15], assumes that the joint PDF $\mathcal{P}_{\rm au}^{\rm f}(a_N^{\rm f}, u)$ factorizes and that large values of κ are associated with small values of u. We extend these arguments, which are similar to those we have given above, to the case of heavy inertial particles to obtain $P_\kappa \sim \kappa^{-5/2}$ and $P_\theta \sim \theta^{-3}$ for their trajectories.

To obtain these exponents accurately from our DNS, we again use the cumulative PDFs Q_κ and Q_θ, which we show in the log-log plots of Figs. 2(a) and 2(b), respectively, for representative values of St. The slopes of the straight-line parts (blue lines) in these plots are $-3/2$ and -2, as expected.

Finally, we compute the mean of the number of points $N_{\rm I}(t,{\rm St})$ at which the torsion changes sign in time t. We find that $N_{\rm I}(t,{\rm St}) \sim t$ for large t, i.e.,

$$n_{\rm I}({\rm St}) \equiv \lim_{t\to\infty} \frac{N_I(t,{\rm St})}{t} \qquad (9)$$

is independent of t; see Fig. 2(c), where we plot $N_{\rm I}/t$ versus time t for two representative values of St. The number $n_{\rm I}({\rm St})$ is a natural measure of the complexity of the particle trajectories and is a function of St alone. We plot $n_{\rm I}({\rm St})$, from our DNSs for several different values of St, in the inset of Fig. 2(c), whence we find that, for large St, $n_{\rm I}$ shows the following scaling behavior:

$$n_{\rm I}({\rm St}) \sim {\rm St}^{-\Delta}, \qquad (10)$$

where $\Delta \simeq 0.5$ (see Ref. [29] for the analog of this result for 2D fluid turbulence). At present, we have not been able to come up with a theory for Δ.

We have shown that various quantities that characterize the geometries of trajectories for heavy inertial particles, advected by a turbulent flow that is homogeneous and isotropic, have PDFs with power-law tails. We have demonstrated this in detail for the PDF of the deviation angle. Furthermore, we have used a similar approach to obtain power laws in the tails of the PDFs of the curvature and torsion. These power laws are not a feature of most other examples of random

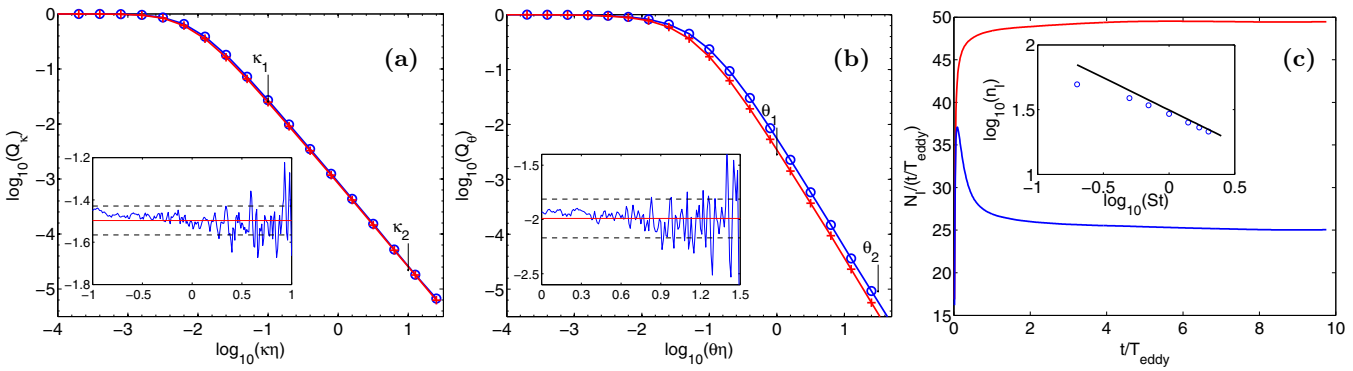

FIG. 2. Cumulative PDFs Q_κ and Q_θ of (a) the curvature κ and (b) the magnitude of the torsion θ of the trajectories of heavy inertial particles for ${\rm St} = 0.2$ (in blue) and ${\rm St} = 1.0$ (in red), obtained by using the rank-order method. The inset shows the values of the local slopes of the tails (a) between κ_1 and κ_2 and (b) between θ_1 and θ_2 for ${\rm St} = 1.0$. (c) Number of points at which the torsion changes sign per unit time [see (9)] as a function of the dimensionless time $t/T_{\rm eddy}$ for ${\rm St} = 0.2$ (red) and ${\rm St} = 1.4$ (blue). The inset shows the plot of $n_{\rm I}$ as a function of St; the straight line in the inset has a slope of -0.5.

curves, which describe physical processes; e.g., a wormlike polymer in thermal equilibrium is also a random curve in three dimensions, but the PDF distribution of its curvature [30] is $P_\kappa \sim \kappa \exp(-\kappa^2)$. Can we conclude, therefore, that the power laws we find are features of turbulence? Our calculations show that the large values of the deviation angle ϕ occur where the fluid velocity becomes very small. However, zeros of the velocity field are not unique to turbulent flows. Therefore, we cannot conclude that the power-law tails in the PDFs we study are unique signatures of the turbulence in the fluid that advects the heavy particles in our study.

We hope that our results will stimulate new experimental [28] and numerical studies of the geometries of inertial-particle trajectories in turbulent flows.

We thank J. Bec, A. Brandenburg, B. Mehlig, E. W. Saw, S. S. Ray, and D. Vincenzi for discussions and particularly A. Niemi, whose study of the intrinsic geometrical properties of polymers [31] inspired our work on particle trajectories. This work was supported in part by the European Research Council under the AstroDyn Research Project No. 227952 (D.M.), Swedish Research Council under Grants No. 2011-542 and No. 638-2013-9243 (D.M.), Knut and Alice Wallenberg Foundation (D.M. and A.B.) under project Bottlenecks for particle growth in turbulent aerosols (Dnr. KAW 2014.0048), NORDITA visiting Ph.D. students program (A.G.), and CSIR, UGC, and DST (India) (A.B., A.G., and R.P.). A.G. thanks the European Research Council (ERC) (Belgium) under the European Community's Seventh Framework Programme (Belgium), ERC Program No. FP7/2007-2013 (Belgium), for support through Grant No. 279004 (DROEMU). We thank SERC for providing computational resources. A.G., P.P., and R.P. thank NORDITA for hospitality under their Particles in Turbulence program; D.M. and M.W. thank the Indian Institute of Science for hospitality and M.W. also thanks the International Centre for Theoretical Sciences, Bangalore.

[1] G. T. Csanady, *Turbulent Diffusion in the Environment* (Springer, Dordrecht, 1973), Vol. 3.
[2] R. A. Shaw, Annu. Rev. Fluid Mech. **35**, 183 (2003).
[3] W. W. Grabowski and L.-P. Wang, Annu. Rev. Fluid Mech. **45**, 293 (2013).
[4] P. J. Armitage, *Astrophysics of Planet Formation* (Cambridge University Press, Cambridge, 2010).
[5] J. Eaton and J. Fessler, Int. J. Multiphase Flow **20**, 169 (1994).
[6] S. Post and J. Abraham, Int. J. Multiphase Flow **28**, 997 (2002).
[7] A. Pumir and M. Wilkinson, Annu. Rev. Condens. Matter Phys. **7**, 141 (2016).
[8] K. Gustavsson and B. Mehlig, Adv. Phys. **65**, 1 (2016).
[9] F. Toschi and E. Bodenschatz, Annu. Rev. Fluid Mech. **41**, 375 (2009).
[10] J. Bec, J. Fluid Mech. **528**, 255 (2005).
[11] F. Toschi, L. Biferale, G. Boffetta, A. Celani, B. J. Devenish, and A. Lanotte, J. Turbul **6**, N15 (2005).
[12] L. Biferale, G. Boffetta, A. Celani, A. Lanotte, and F. Toschi, Phys. Fluids **17**, 021701 (2005).
[13] W. Braun, F. De Lillo, and B. Eckhardt, J. Turbul. **7**, 1 (2006).
[14] H. Xu, N. T. Ouellette, and E. Bodenschatz, Phys. Rev. Lett. **98**, 050201 (2007).
[15] A. Scagliarini, J. Turbul. **12**, 571261(2011).
[16] C. Canuto, M. Y. Hussaini, A. Quarteroni, and T. A. Zang, *Spectral Methods in Fluid Dynamics* (Springer, Berlin, 1988).
[17] A. G. Lamorgese, D. A. Caughey, and S. B. Pope, Phys. Fluids **17**, 015106 (2005).
[18] G. Sahoo, P. Perlekar, and R. Pandit, New J. Phys. **13**, 013036 (2011).
[19] R. Gatignol, J. Mec. Theor. Appl. **2**, 143 (1983).
[20] M. R. Maxey and J. J. Riley, Phys. Fluids **26.4**, 883 (1983).
[21] M. Spivak, *A Comprehensive Introduction to Differential Geometry* (Publish or Perish, Berkeley, 1979), Vols. 1–5.
[22] M. Stone and P. Goldbart, *Mathematics for Physics: A Guided Tour for Graduate Students* (Cambridge University Press, Cambridge, 2009), p. 242.
[23] U. Frisch, *Turbulence* (Cambridge University Press, Cambridge, 1996).
[24] A. N. Kolmogorov, Dokl. Akad. Nauk. SSSR **30**, 9 (1941).
[25] L. Biferale, G. Boffetta, A. Celani, B. J. Devenish, A. Lanotte, and F. Toschi, Phys. Rev. Lett. **93**, 064502 (2004).
[26] Kolmogorov's theory [24] predicts that the PDF of the acceleration components is a stretched exponential, i.e., $P_{\rm a}^{\rm f}(y) \sim y^\alpha \exp(-y^\beta)$, with $\beta = 8/9$ for large y; see, e.g., Ref. [25]. If we assume the stretched-exponential form then for $\phi \ll 1$ we can integrate Eq. (6) to obtain $P_\phi \sim \phi^\alpha$ even for $\phi < \phi_*$. Note, however, that the numerical data for $P_{\rm a}^{\rm f}(y)$ is better described by the multifractal model, which takes intermittency into account, yielding a more complex expression for $P_{\rm a}^{\rm f}(y)$ as a sum of the stretched exponential with certain weights [25].
[27] D. Mitra, J. Bec, R. Pandit, and U. Frisch, Phys. Rev. Lett. **94**, 194501 (2005).
[28] When we first presented our results, E. W. Saw checked whether his experimental data were consistent with our results. His analysis, which used a variable akin to, but not the same as, ϕ, does have a PDF with a tail characterized by an exponent $\simeq -4$, in agreement with our result.
[29] A. Gupta, D. Mitra, P. Perlekar, and R. Pandit, arXiv:1402.7058.
[30] S. M. Rappaport, S. Medalion and Y. Rabin, arXiv:0801.3183.
[31] S. Hu, M. Lundgren, and A. J. Niemi, Phys. Rev. E **83**, 061908 (2011).